Srđan M. Bošnjak
Professor emeritus
University of Belgrade
Faculty of Mechanical Engineering

Dejan B. Momčilović
Associated research professor
University of of Belgrade
Innovation Center of the Faculty of Mechanical Engineering

Nebojša B. Gnjatović
Assistant professor
University of Belgrade
Faculty of Mechanical Engineering

Aleksandar Z. Stefanović
Teaching assistant
University of Belgrade
Faculty of Mechanical Engineering

Marko M. Urošević
Research assistant
University of Belgrade
Faculty of Mechanical Engineering

Ivan Lj. Milenović
Senior Technical Associate
University of Belgrade
Faculty of Mechanical Engineering

Corrosion-provoked Collapse of the Inclined Belt Conveyor Bridge

This paper presents the results of the holistic failure-based root cause analysis of a sudden collapse of the inclined belt conveyor bridge (IBCB), which is a vital subsystem of a steel mill raw material handling system. Through a comprehensive analysis of the set of possible causes ('design-in' defects, 'manufacturing-in' defects, 'exploitation-in' defects and 'environmental-in' defects), by the method of elimination it has been determined that the inadequate maintenance of the anti-corrosion coating was the root cause of collapse of the IBCB. Due to inadequate maintenance of the anti-corrosion coating of the IBCB structure, heavy and uniform corrosion, provoked by increased acidity of precipitations in the area of the steel mill, had led to disintegration of structural elements and, ultimately, collapse of the IBCB structure. Additionally, based on the appearance and position of the collapsed remains of the IBCB, as well as state of the objects connected by it before the breakdown, the structural collapse scenario was established. Results of the presented investigation underline the importance of the corrosion inspection and monitoring, especially in cases of facilities exposed to chemically aggressive environments. The expenses of planned standstills for the purpose of corrosion inspection and potential repairs on the structural elements damaged by corrosion are significantly lower than direct and indirect expenses of by accidental destruction.

Keywords: *Inclined belt conveyor bridge, collapse, root cause analysis, inadequate maintenance, corrosion, structural collapse scenario*

1. INTRODUCTION

Belt conveyor bridges are widely used in the extraction and processing of raw materials [1-3]. Depending on the environments they are servicing, belt conveyor bridges can be mobile or stationary. Given the fact that the systems for extraction and processing of raw materials are typically characterized by the serially coupled subsystems, failures of the belt conveyor bridges lead to downtimes of said subsystems as a whole. In addition to direct material costs, failures of structural elements [4-8] and their damage caused by the loss static stability [9] or extreme environmental conditions (such as wind) [10], as well as failures of vital mechanical components [11-14] and the conveyor belt [15-17], also lead to indirect financial losses due to the standstill in pro–duction. Considering that these are, as a rule, high-ca–pacity systems, said indirect financial losses are, typically, significantly higher than direct costs [18,19].

The inclined belt conveyor bridge (IBCB), with the inclination angle of 15.2°, Fig. 1, which represents a vital transport subsystem of a steel mill and connects the primary ore mixing plant (4), which also houses the transfer point 4, with the agglomeration plant (5), was put into exploitation in 1971. The IBCB was designed as a three-span (segments 3.1, 3.2 and 3.3) lattice space structure (width of 6.25 m, height of 2.6 m, total length of 108 m) with corrugated sheet metal cladding. Its support columns (C1 and C2) were designed as plane lattice structures, with the height of column C1 of 17 m, and the height of column C2 of 26.45 m. Inside the IBCB, two identical belt conveyors (BC A1 and BC A2, belt width of 1200 mm, designed capacity of 600 t/h) were placed side by side.

Following the sudden breakdown of the structure of the IBCB, Fig. 1 (Details A–I), thorough investigations were conducted with the goal of determining the cause of the complete collapse. This paper presents the results of: (i) visual examinations (both, in situ and in labo–ratory) of the collapsed structure; (ii) experimental in–vestigations conducted on the samples taken from the representative structural elements (chemical analyses, tensile and impact tests, microhardness, as well as me–tallographic examinations); (iii) analysis of the referent working regimes of the BCs; (iv) analysis of the meteorological and seismic data; (v) analysis of the project documentation and the control (periodic) geo–detic recordings of the construction during exploitation. By the means of a comprehensive analysis of the set of possible causes ('design-in' defects, 'manufacturing-in' defects, 'exploitation-in' defects and 'environmental-in' defects) and a method of elimination, the root cause of collapse of the IBCB was determined. Additionally, based on the appearance and position of the broken remains of the IBCB structure, as well as the conditions of the objects (facilities) it was connecting prior to the accident, the structural collapse scenario was estab–lished. Based on the analysis of the results of the invest-

Received: August 2025, Accepted: September 2025
Correspondence to: Srđan Bošnjak
Faculty of Mechanical Engineering,
Kraljice Marije 16, 11120 Belgrade 35, Serbia
E-mail: sbosnjak@mas.bg.ac.rs
doi: 10.5937/fme2504639B

Figure 1. Layout of the inclined belt conveyor bridge and its state after the collapse: 1-column C1; 2-column C2; 3-three-segment belt conveyor bridge (segments 3.1, 3.2 and 3.3); 4-primary ore mixing plant, where the transfer point 4 is located; 5-agglomeration plant; 6-inclined belt conveyor R5-1 bridge; 7-radial precipitator; 8-transfer point 5.

igations, using the original methodology, the root cause of the collapse of the IBCB structure was determined. The holistic failure-based root cause ana–lysis presented in this paper has a broader significance due to the capability of its application in solving the analogous problems which occur in many engineering objects, facilities and systems [20-22].

2. VISUAL EXAMINATIONS

2.1 Visual examinations on site

The first visual examination was conducted immediately after the accident. It was then determined that the seg–ment 3.1 of the IBCB was fractured during the break–down, Fig. 1 (Detail A), whereas its starting segment had remained connected to the primary ore mixing plant, Fig 1 (Detail B). Part of the segment 3.2 which was continuing from the segment 3.1, remained con–nected to the column C1, Fig. 1 (Detail C), whereas the remainder of the segment 3.2 broke off and was in the radial precipitator afterwards, Fig. 1 (Detail D), as was the column C2 (Detail G). During the fall, Fig. 1 (Detail E), the segment 3.3 of the IBCB had collided with the inclined belt conveyor R5-1 bridge, which had caused the collapse of its segment between the support column and the transfer point 5, Fig. 1 (Detail F).

After the site of the accident was cleared, the second visual examination of the remnants of the collapsed IBCB structure was conducted. On this occasion, heavy corrosion was observed on all elements, accompanied by the complete disintegration of the structural parts, Fig. 2. The visual examination did not find any signs of settling of the concrete foundations of the columns, Fig. 3, nor a pronounced corrosion of the anchor bolts and, instead, the parts of the foundations broke off during the breakdown, Fig. 3 (b,c). Unlike the very pronounced corrosion of the structural elements, clas–sified as C5-I [23], no high corrosion damage of the bolted joints was found on the available segments of the broken load bearing structure, Fig. 4.

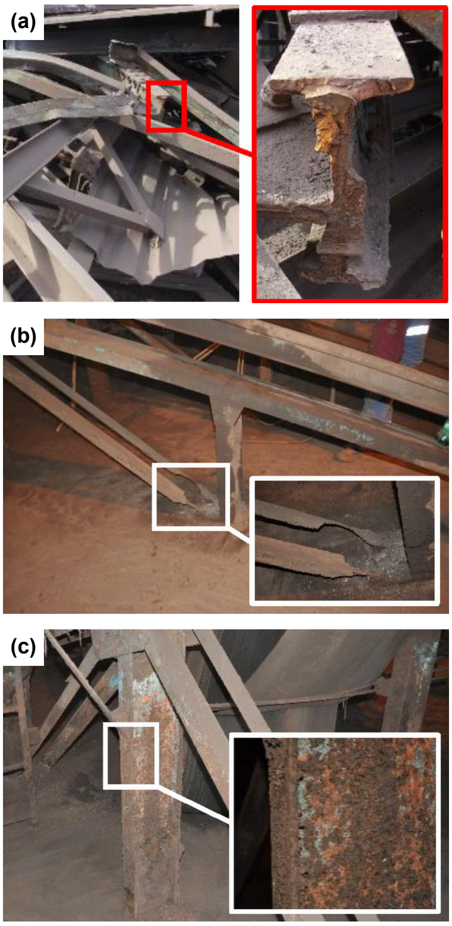

Figure 2. Details of the fractured element of the lower truss of the IBCB structure (a), diagonal segment (b) and the column (c) of the load bearing structure of the belt conveyor drive station at the transfer point 4.

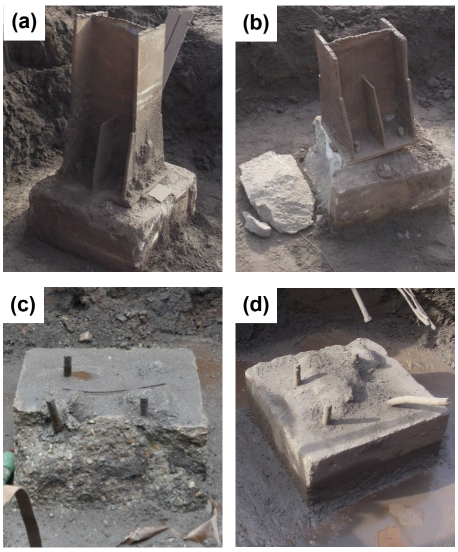

Figure 3. The left (a) and right (b) foundations and foots of the column C1; the left (c) and right (d) foundations of the column C2.

High corrosion intensity, Fig. 5(a), as well as heavy deposits of agglomerate, Fig. 5(b), were observed on the load bearing structure of a IBCB located in close proximity to the collapsed IBCB.

The representative structural parts selected for the laboratory visual examinations and characterization of materials used in manufacturing of the collapsed IBCB structure are shown in Fig. 6.

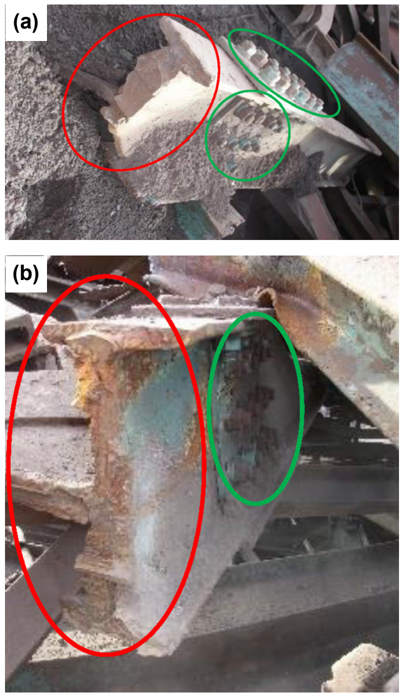

Figure 4. Local corrosion intensity - bolted joints vs structural elements: (a) hot rolled IPN 240 beam of the lower truss; (b) hot rolled IPN 160 beam of the upper truss.

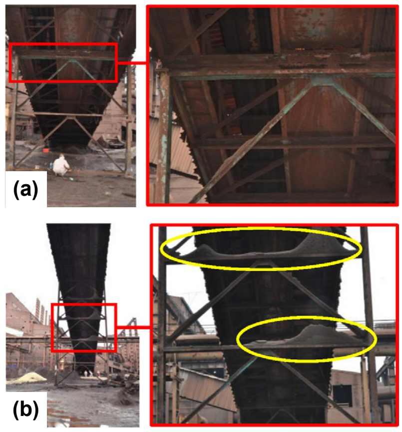

Figure 5. (a) High corrosion intensity of the load bearing structure of the neighboring IBCB; (b) heavy deposits of agglomerate.

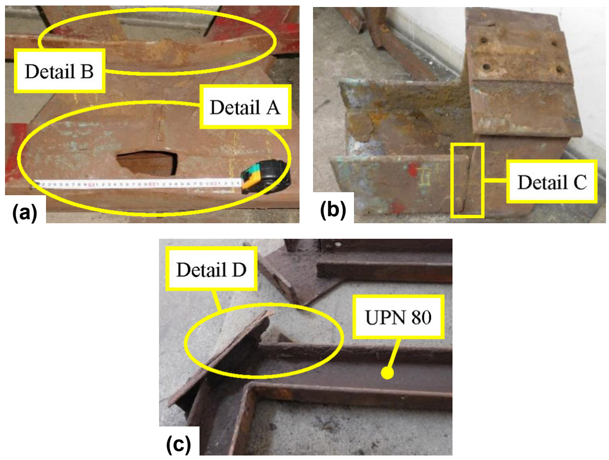

Figure 6. Representative structural parts of the collapsed IBCB: (a) a part of the box section of the lower truss, made from two rolled channels UPN 160 (Detail A) and a hot rolled angle L 65×65×7 (Detail B); (b) a part of the structure of the column C1; (c) a part of the girder made from hot rolled channel UPN 80.

2.2 Laboratory visual examinations

Before the samples were taken for the experimental investigations of the material, a visual inspection was performed on the parts of the structure obtained for the tests. Apart from plastic deformation of the box section girder (2×UPN 160 hot rolled channel) of the lower truss, Fig. 6(a) (Detail A), and the hot rolled angle L 65×65×7, Fig. 6(a) (Detail B), a fracture of a part of the flange of the UPN 160 channel and the single butt weld cracking, Fig. 7(a), as well as incomplete root penetration of the said weld, Fig. 7(b), were also observed. In case of column C1, welding defects of the type incomplete root penetration and cracks, Fig. 8(a), as well as welding undercuts, Fig. 8(b), were also detected. Additionally, a very intensive and uniform corrosion was observed, which had led to the total local disintegration of certain structural elements, Fig. 6(c) (Detail D).

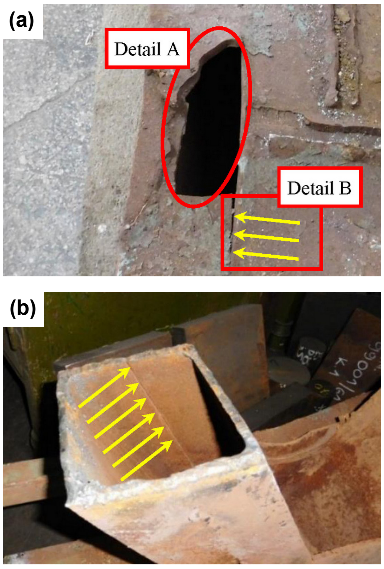

Figure 7. Details of the box girder (2×UPN 160 channel) of the lower truss of the belt conveyor bridge: (a) fracture of the part of the flange and the single butt weld cracking; (b) incomplete root penetration of the single butt weld.

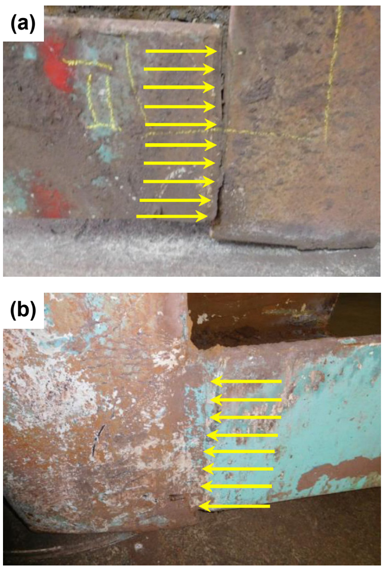

Figure 8. Welding defects of the column C1: (a) incomplete root penetration and cracks (Detail C in Fig. 6(b)); (b) undercuts.

3. EXPERIMENTAL INVESTIGATIONS

Chemical composition, Table 1, was determined with the OES instrument Belec Lab 3000S [24,25]. Deter–mination of the tensile properties, Table 2, was conduc–ted in accordance with the standard [26]. The impact energy tests [27] were performed on the specimens with reduced section width of 7.5 mm and 5 mm, Table 3.

Based on the results presented in Tables 1–3, the following can be concluded:

- the material of the samples 1 (UPN 160 channel) and 3 (UPN 80 channel) closely matches the quality class of steel S235J2 [28], whereas the material of the sample 2 (angle L 65×65×7) most closely matches the quality class of steel S275J2 [28];
- the experimentally determined values of elongation and impact energy unquestionably confirm that the materials of the tested elements are highly ductile, i.e. possess a large reserve of plasticity.

The specimen for metallography examination, Fig. 9(a), was taken from the single butt weld area of flanges of two profiles UNP 160, Fig. 7(b), where no fracturing of the welded connection had occurred. On the same specimen, microhardness (HV1) testing was also conducted, in accordance with the standard [29], Fig. 9(b). The average measured microhardness value of the parent metal is 132 HV1, Table 4, which is in compliance with the data given in [30] for quality class of steel S235J2 used to manufacture the profiles UNP 160. The average measured microhardness value in the heat-affected zone (142 HV1), as well as the average measured microhardness value of the weld metal (184 HV1) are also within the expected boundaries. If, in accordance with the expressions given in [31], the ultimate tensile stress and the yield stress values are calculated based on the value of average measured microhardness, Table 4 (parent material), the following is obtained:

$$\sigma_{UTS,HV} = -99.8 + 3.8 H_V = = -99.8 + 3.8 \times 132 = 402 \text{ MPa}, \tag{1}$$

$$\sigma_{YS,HV} = -70.5 + 2.736 H_V = = -70.5 + 2.736 \times 132 = 291 \text{ MPa}. \tag{2}$$

The ultimate tensile stress determined in such a way, for the adopted accuracy of calculation of averaged mechanical characteristics, is equal to the average measured ultimate tensile stress for the sample 1, Table 2, whereas the calculated yield stress deviates by

$$\sigma_{UTS,HV} = 100\left(\sigma_{YS,HV} - \sigma_{YS,S1}\right) / \sigma_{UTS,S1} = = 100\left(291 - 280\right) / 280 \approx 4\%, \tag{3}$$

which attests to the good mutual compliance of the measurements of tensile properties and microhardness.

Metallographic examination of the specimen (area marked with MTG in Fig 9(b)), conducted by optical light microscope, revealed a crack in the weld metal, caused by very intensive corrosion, Fig. 10

Table 1. Chemical analysis (wt.%)

Sample	C	Si	Mn	P	S	Cr	Ni	Al	Mo
1[a]	0.133	0.107	0.35	0.021	0.033	0.006	0.016	0.004	0.005
2[b]	0.066	0.008	0.32	0.047[d]	0.031	<0.002	0.018	0.013	0.052
3[c]	0.122	0.013	0.42	0.011	0.0044	0.004	0.023	0.007	0.006
S235J2 [28]	max. 0.19	-	max. 1.5	max. 0.035	max. 0.035	-	-	-	-
S275J2 [28]	max. 0.21	-	max. 1.6	max. 0.035	max. 0.035	-	-	-	-

[a]Hot rolled channel UPN 160: Fig 4(a) (Detail A); [b]Hot rolled angle L 65×65×7: Fig 4(a) (Detail B);
[c]Hot rolled channel UPN 80: Fig 4(c); [d]Usual out of range content for the steel produced more than 50 years ago

Table 2. Tension test results

Sample	Specimen	Yield stress (MPa)		Ultimate tensile strength (MPa)		Ratio of the yield strength to the tensile strength		Elongation (%) $L_0=5.65S_0^{1/2}$	
		σ_{YS}	average	σ_{UTS}	average	$r_{YS/UTS}$	average	A	average
1	1	278	280	405	402	0.68	0.69	29.8	28.9
	2	286		397		0.72		27.8	
	3	275		403		0.68		29.2	
2	1	327	316	420	416	0.78	0.76	28.5	38.4
	2	309		411		0.75		28.1	
	3	313		418		0.75		28.5	
3	1	305	301	363	358	0.84	0.84	29.5	29.1
	2	301		360		0.83		29.5	
	3	296		351		0.84		28.2	
S235J2 [28]		min. 235		min. 360		-		min. 26	
S275J2 [28]		min. 275		min. 410		-		min. 23	

Table 3. Impact energy test results

Sample	Specimen	Width (mm)	Temperature (°C)	Impact energy $KV_{300/2}$ (J)	Average (J)	Average reduced to specimen cross-section 10×10 mm (J) [28]
1	1	7.5	+20	55.9	55.2	73.6
	2			53.9		
	3			55.9		
	4		0	50.0	51.3	77.0
	5			50.0		
	6			53.9		
	7		–20	45.1	44.4	66.6
	8			43.1		
	9			45.1		
2	1	5	+20	51.9	50.9	101.8
	2			51.9		
	3			49.1		
	4		0	43.1	41.8	83.6
	5			41.2		
	6			41.2		
	7		–20	38.2	37.9	75.8
	8			37.3		
	9			38.2		
3	1	5	+20	39.2	37.6	75.2
	2			35.3		
	3			38.2		
	4		0	37.3	35.9	71.8
	5			35.3		
	6			35.3		
	7		–20	33.3	33.9	67.8
	8			35.3		
	9			33.3		
S235J2, S275J2 [28]		10	–20	-	-	min. 27

Table 4. Microhardness test (HV1) results

Measuring points	Microhardness HV1		
	minimal	maximal	average
Parent metal	125	140	132
Heat-affected zone	135	148	142
Weld metal	182	189	184

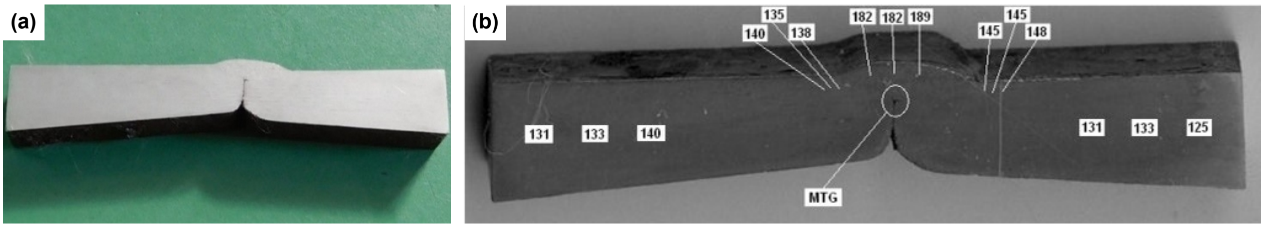

Figure 9. (a) Metallographic specimen; (b) microhardness HV1 [26] and position (MTG) for metallographic examination of the single butt weld.

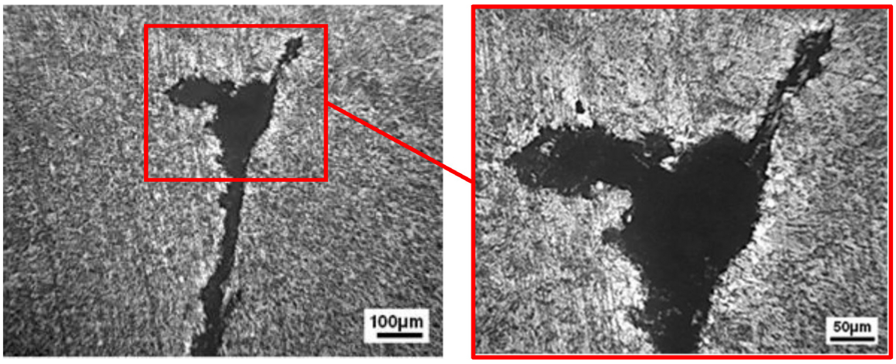

Figure 10. Crack initiation in the weld metal.

4. REFERENT WORKING REGIMES OF THE BELT CONVEYORS

According to the maintenance log and the work log, throughout the entire exploitation period: (i) pronounced vibrations of the IBCB structure, as a potential conse–quence of the imbalance of the rotating masses of the BCs, were not observed; (ii) the BCs did not operate in the overload regimes. According to the same sources, over a two-month period before the collapse, the ave–rage capacities of the BCs were 153 t/h (BC A1) and 167 t/h (BC A2). This means that, in the said period, the average load the IBCB structure, caused by the weight of the conveyed material, was at the level of 100 ×153/600=26% (BC A1) i.e. 100×167/600=28% (BC A2) of the said load at the designed capacity (600 t/h). At the moment of breakdown, the capacity of the BC A1 was 36 t/h, i.e. 6% of the designed capacity, whereas the BC A2 was working in the idle operation regime.

5. ENVIRONMENTAL CONDITIONS

One of the possible causes of the collapse of the IBCB structure, in principle, can also be the extreme impact of the environment.

For the micro-location of the steel mill and the referent period (day of the collapse and 10 days prior), the following extreme values of meteorological conditions can be singled out as referent for further analysis:

- the minimum temperature in the referent period: t_{min}=–13.4 °C, measured on the day before the collapse;
- the minimum temperature on the day of the collapse: $t_{min,a}$=–5.6 °C;
- the maximum height of the snow layer in the referent period was measured on the day of the collapse: $h_{s,max}$=$h_{s,a}$=18 cm;
- the maximum wind velocity (measured two days before the collapse): $v_{w,max}$=20.7 m/s;
- the maximum wind velocity on the day of the collapse: $v_{w,max,a}$=4.8 m/s.

According to the seismological reports, over the entire period of exploitation, no earthquakes which could jeopardize the integrity of the IBCB structure were registered.

A highly pronounced and even corrosion (Section 2), is the consequence of the increased acidity of precipitations in the area of the steel mill. Namely, every activity in the integrated steel mill (mixing of raw materials, sintering, blast furnace, converting and casting) produces fumes and dust with known basic chemical composition [32-34]. Chemical and physical properties of the dust and fumes generated by the regular production in integrated steel mills, have been discussed mainly from the standpoint of emission control [32] and public health issues [33]. However, the gases in steel mills with increased content of compounds like CO_2, SOx, NOx, H2S, HCl etc., also have a significant negative effect by promoting corro–sion in the presence of moisture on various steel mill elements [34].

This means that the regular atmospheric corrosion is more pronounced in the presence of fumes containing said compounds and particles present in steel mills, due to the increased level of acidity of local precipitations. This effect also contributes to the accelerated forming of a corroded layer which, after formation, actually provides protection against the environment in general, but also adds a layer of complexity to the electro-chemistry of the corrosion process. The fact that the rust formed on the corroded surface of the investigated steel grade consists of two layers, the inner and the outer, had led to successive phases of rust forming, followed by the decreased rate of corrosion and falling off of the outer rust layer and breaking of the inner rust layer with the corrosion rate increase, which had led to propagation of corrosion and could cause structural failure [35-37].

6. ANALYSIS OF THE PROJECT DOCUMENTATION AND GEODETIC SURVEYS

The project the IBCB structure is in full compliance with the demands of the technological process and the technical regulations which was in effect at the time of its manufacture (1970.). The project-defined materials of the structural elements (which correspond to steels of the quality classes S235J2 and S275J2), as well as all of the applied constructional solutions, are typical for this type of steel bearing structures. The load analysis encompassed the impacts of both the main and the additional loads. According to the project, the IBCB structure fully meets the criteria of strength, stiffness and elastic stability.

Regarding the additional loads of the IBCB structure, the impact of wind was accounted for with the basic wind load of w_0=883 N/m^2, which corresponds to the wind velocity of [38]

$$v_{\mathrm{w},0}=\sqrt{\frac{w_0}{0.613}}=\sqrt{\frac{883}{0.613}}=37.95\ \frac{\mathrm{m}}{\mathrm{s}}=136.6\ \frac{\mathrm{km}}{\mathrm{h}}. \quad (4)$$

Over the referent period, the highest wind velocity was registered two days before the collapse (Section 5), and was $v_{\mathrm{w,max}}$=20.7 m/s, which is $v_{\mathrm{w},0}/v_{\mathrm{w,max}}$ = 37.95/20.7=1.9 times lower than the wind velocity corresponding to the calculational basic wind load. On the day of the collapse, the maximum recorded wind velocity (Section 5) $v_{\mathrm{w,max,a}}$=4.8 m/s was lower than the wind velocity which corresponds to the basic wind load by $v_{\mathrm{w},0}/v_{\mathrm{w,max,a}}$=37.95/4.8=7.9 times.

The calculation of the IBCB structure also accounted for the impact of snow, where the adopted basic uniform snow load was $q_{\mathrm{s},0}$=0.75 kN/m^2. The snow layer started to form two days before the breakdown. On the day of the breakdown, its height was (Section 5) $h_{\mathrm{s,a}}$=$h_{\mathrm{s,max}}$=18 cm. According to [39], the weight density of snow settled for several days is γ_{s}=2.0 kN/m^3. Starting from the weight density adopted in such a manner, it is concluded that, on the day of the accident, the basic uniform snow load was

$$q_{\mathrm{s,a}}=\gamma_{\mathrm{s}}h_{\mathrm{s,a}}=2.0\times0.18=0.36\ \frac{\mathrm{kN}}{\mathrm{m}^2}, \quad (5)$$

which is $q_{\mathrm{s},0}/q_{\mathrm{s,a}}$=0.75/0.36=2.1 times lower than the calculational basic uniform snow load.

According to the results of the geodetic recordings, performed after the assembly and periodically during exploitation, the deviations of the geometry of the IBCB structure were within the permitted boundaries.

7. DISCUSSION

According to [40], the potential causes of the break–down of the IBCB structure can be categorized in four fundamental groups:

- defects that occurred during the design of the load bearing structure, i.e. the so called 'design-in' defects – defects of the type D1 (D1.1: selection of material; D1.2: selections of constructional solutions; D1.3: identification of loads, i.e., the stress-strain state and the elastic stability);
- defects that occurred during the manufacturing of the load bearing structure, the so called 'manufacturing-in' defects – defects of the type D2 (D2.1: production of the built-in materials and profiles; D2.2: manufacture of connections of the elements of the structure; D2.3: assembly);
- defects that occurred during the exploitation, the so called 'exploitation-in' defects – defects of the type D3 (D3.1: operating; D3.2: maintenance);
- extreme effects of the environment, the so called 'environmental-in' defects – defects of the type D4 (D4.1: wind; D4.2: snow; D4.3: temperature; D4.4: earthquake; D4.5: settling of the ground; D5.5: corrosion).

Based on the detailed analysis of the project of the IBCB structure and on the basis of the results of the analyses presented in Section 6, it is concluded that the selection of the material, the constructional solutions, as well as calculation of the IBCB structure, are fully compliant with the level of technical knowledge and regulations that were in effect at the time of manufacturing of the facility. Therefore, the defect of the type D1 is excluded from the set of possible causes of the collapse of the IBCB structure.

Based on the results of the examination of the chemical composition and mechanical characteristics of the used materials (Section 3), it is concluded that they fully meet the demands of the project and the standard [28], i.e. the defect of the type D2.1 is excluded as the possible cause of the collapse. The incomplete root penetration (Section 3), with simultaneous negative effect of the corrosion, can lead to the propagation of the crack. However, during exploitation, the IBCB structure was not exposed to pronounced dynamic loads (Section 4) and, therefore, it can be claimed, with high degree of likelihood, that the defects that occurred during the creation of the welded joints were not the root cause of the collapse. Furthermore, the visual examination did not determine failures of bolted joints, meaning that neither the defects of the type D2.2 were the cause of the collapse of the IBCB structure. Given the fact that throughout the entire period of exploitation, the geometric deviations of the IBCB structure were within the allowed boundaries (Section 5), it is concluded that the eventual defect of the type D2.3 is certainly not the cause of the collapse.

Over the two-month period preceding the collapse, as well as the moment of the breakdown, the working loads of the inclined belt-conveyor bridge caused by the weight of the conveyed material were considerably lower than the designed values (Section 4), which excludes the defect caused by the handling of the mechanical subsystem (defect of the type D3.1) from the set of possible causes of the collapse. On the other hand, the heavy corrosion, described in Section 2, accompanied by the total local disintegration of the elements of the load bearing structure of the collapsed IBCB, as well as pronounced corrosion on the load bearing structure of the neighboring IBCB, lead to the conclusion that the defect caused by the inadequate maintenance of the anti-corrosion coating (defect of the type D3.2) had enabled the corrosion-induced weakening of the collapsed IBCB structure. Pronounced deposits of the foreign material (also the defect of the type D3.2), observed on the structure of the neighboring IBCB (Section 2), intensify the destruction effect of corrosion and induce increased loading of the structural elements.

Values of the basic wind and snow loads, which were adopted as the foundation for the load analysis and the proof of strength of the collapsed IBCB structure, are significantly higher that the values of said loads over the entire referent period (Section 6). This excludes the possibility that the defects of the type D4.1 and D4.2 could have led to the collapse of the IBCB structure. The results of the impact energy tests (Section 3), as well as data on the temperature stated in the meteorological log (Section 5), exclude the possibility that the impact of the environmental temperature on the mechanical characteristics of the material (defect of the type D4.3) had led to the breakdown. Neither over the referent period, nor the entirety of exploitation, no extreme movement of the ground caused by earthquake had occurred (Section 5), which excludes the possible impact of the defect of the type D4.4. Based on the control geodetic recordings of the load bearing structure (Section 6) and the visual examination after the breakdown (Section 2), it is concluded that the settling of the foundations of the columns, i.e. the defect of the type D4.5, was not the cause of the breakdown.

Based on the presented analyses and having in mind the fact that the observed defects in the manufacture of the welded joints of the structural elements were not present in the degree that would lead to the breakdown in the regular regime of exploitation and maintenance, it is concluded that the inadequate maintenance of the anti-corrosion coating, i.e. the defect of the type D3.2, was the root cause of the collapse of the IBCB structure. This defect had allowed the formation and propagation of the environ–mental-in defect of the D5.5 type (corrosion), i.e. the disintegration of the constructional elements caused by the heavy and uniform corrosion which had led to: (i) drastic reduction of the cross-sectional areas of the structural elements followed by the increase of the stress; (ii) reduc–tion of the fatigue strength [41]. Recent research results emphasize that, for the global corrosion case, the reduction factors of the yield resistance and the ultimate resistance of a beam are linearly and negatively correlated with the corrosion ratio [42,43]. As the corrosion time increased, the yield load, the ultimate load, and the ulti–mate displacement of the corroded specimens decreased signifi–cantly [44]. In the case of local corrosion, the formation of stress concentration features can lead to significant increase of the stress concentration factor, which can range from 3.3 to 7.5 [45]. However, in cases of either random or localized corrosion, the possibility of element failure is dependent on the location of the corrosion and the local geometry fea–tures, such as welding and other manufacturing defects [46]. Long-term research of corrosion in the steel mill reveals that the steel structures have suffered severe corrosion damage, emphasizing the necessity of urgent assessment of structural safety and reliability [47]. In facilities with similar maintenance problems [48] and levels of complexity, recent developments in artificial intelligence (AI) create promising opportunities to revolutionize the corrosion monitoring process and optimize the maintenance program [49,50].

Scenario of the IBCB collapse

Although the collapse had occurred before noon, there were no direct witnesses nor surveillance cameras. The process of the collapse was reconstructed based on the appearance and position of the broken remains of the collapsed IBCB, the state of the object it was connecting (the primary ore mixing plant and the agglomeration plant), as well as state of the inclined belt conveyor R5-1 bridge, Figs. 1 and 11.

Based on the facts that: (i) the no damages that would point to the impact of the IBCB segment 3.3, Fig. 1 (Details C and F), were observed on the face of the agglomeration plant; (ii) after the collapse, the longitudinal direction of said segment, Fig. 1 (Detail E), corresponds to its direction before the collapse, Fig. 11(a) – direction: primary ore mixing plant (4) → agglomeration plant (5) – which means that during the collapse it was moving in practically the same vertical plane it was in before the breakdown; (iii) a segment of the inclined belt conveyor R5-1 bridge, Fig. 1 (Details E and F), which was located immediately below the IBCB segment 3.3, Figs. 1 and 11(a), had also collapsed during the breakdown; it can be concluded that the collapse of the IBCB was triggered by the corrosion-caused jeopardized integrity of the bottom chord of the segment 3.3 in close proximity of the support C, Fig. 11(b). After breaking off, the segment 3.3 had started rotating around the support D located in the agglomeration plant, Fig. 11(b), separated from it, fell and struck the inclined belt conveyor R5-1 bridge, collapsing its segment between the column and the transfer point 5, Fig. 1 (Detail E). By hitting the inclined belt conveyor R5-1 bridge, the segment 3.3 was deflected towards the column C2, Fig. 11(b). The im–pact of the segment 3.3 had caused plastic deformation of the column C2 and shearing of the screw connection in the support C, Fig. 11(c), whereas segment 3.3 was deflected towards the agglomeration plant and fell to the ground, between the plant and the radial precipitator, Fig. 1 (Detail E). The weight of the segment 3.2 had caused further bending of the column C2, which was accompanied by: (i) leaning of the column C2 onto the concrete construction of the radial precipitator and its total bending plastification, Fig. 1 (Detail G), as well as column foots being torn away from the concrete foundations, Fig. 1 (Detail H); (ii) rotation of the segment 3.2 around the support B, Fig. 11(c), bending of the column C1 until it rested on the radial preci–pitator, Fig. 1 (Detail I) and fracturing of the segment 3.2 into two parts. Its starting part, after falling into the radial precipitator, remained connected to the column C1, Fig. 1 (Detail C) and Fig. 11(c), whereas its ending part, which was resting on the column C2, also ended up in the radial precipitator, Fig. 1 (Detail D). At the same time, due to the bending of the column C1, the segment 3.1 had lost its right support (B), Fig. 11(c), and started rotating around the support A (fixed point of the belt conveyor bridge structure) located in the transfer point 4 building, and broke into two parts after falling onto the ground, Fig. 1 (Detail A). Its starting part remained connected to the primary ore mixing plant. The configuration of the IBCB after the collapse is shown in Fig. 11(d).

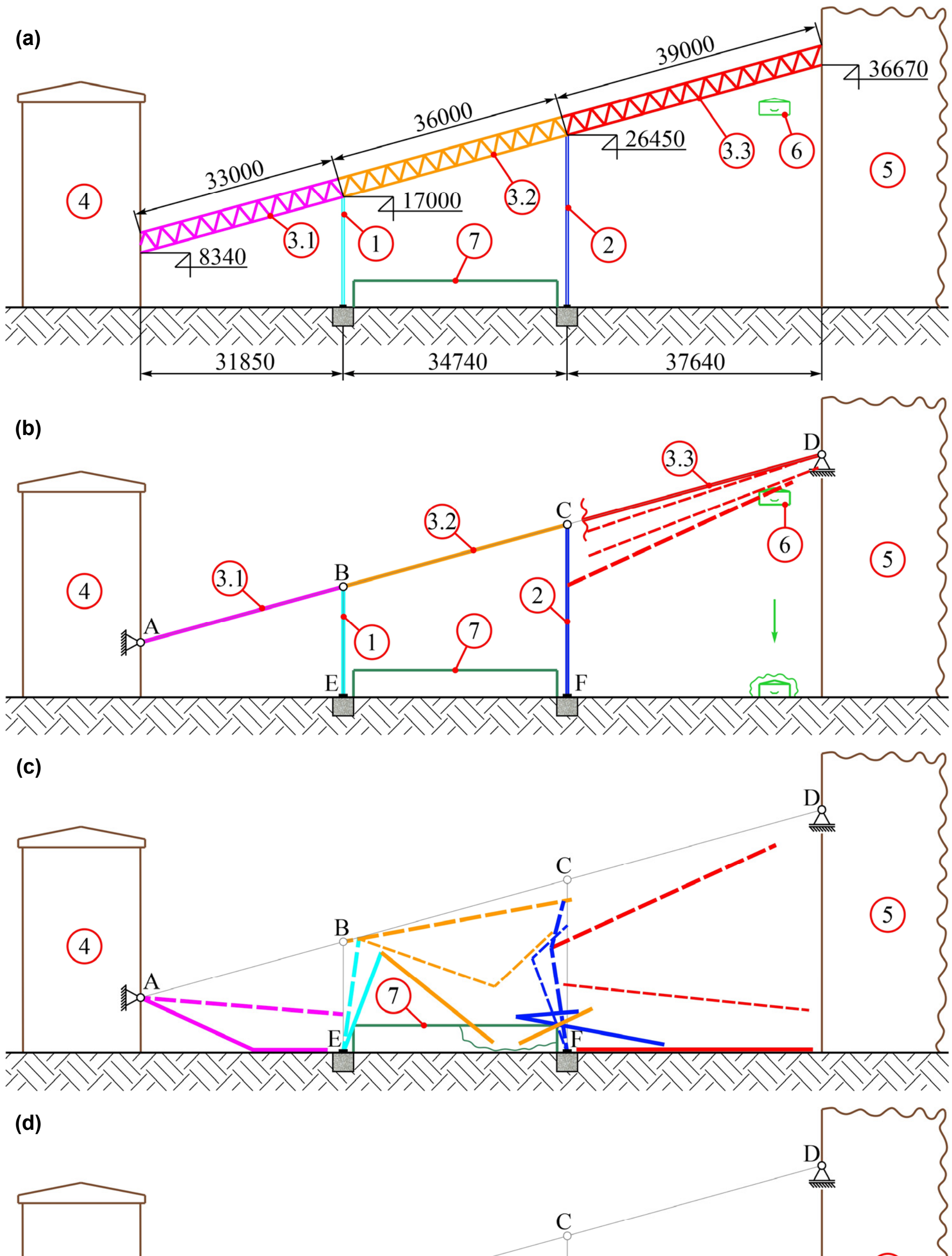

Figure 11. Layout of the inclined belt conveyor bridge (a) and the main stages of the breakdown (b,c,d): 1-column C1; 2-column C2; 3-three-segment belt-conveyor bridge (segments 3.1, 3.2 and 3.3); 4-primary ore mixing plant, where transfer point 4 is located 4; 5-agglomeration plant; 6-inclined belt-conveyor R5-1 bridge; 7-radial precipitator; 8-transfer point 5; A, D: end supports of the IBCB; B, C-intermediate supports of the IBCB, i.e. heads of the columns C1 and C2; B_1, C_1: position of the heads of the columns C1 and C2 after the collapse ; E, F: foots of the columns C1 and C2; F_1: position of the C2 foots after the collapse.

8. CONCLUSION

This paper presents the results of key stages of the investigation on the cause of the collapse of the 108 m long inclined belt conveyor bridge (IBCB), which is a vital transport subsystem of a steel mill. Based on the analysis of the results of visual examinations and the characterization of materials, as well as the analysis of the referent working regimes of the belt conveyors, meteorological and seismic data, project documentation and the control geodetic recordings of the IBCB structure during the exploitation, it was determined that the inadequate maintenance of the anti-corrosion coa–ting is the root cause of collapse of the IBCB. As a con–sequence, heavy and uniform corrosion, provoked by the increased acidity of precipitations in the area of the steel mill, had led to the disintegration of structural elements and, finally, the collapse of the IBCB struc–

ture. Additionally, based on the visual state and the position of the collapsed remains of the IBCB, as well as the state of the objects connected by it before the breakdown, the structural collapse scenario was esta–blished.

The results of the presented investigation underline the importance of corrosion inspection and monitoring, especially in case of the facilities exposed to the impact of a chemically aggressive environment. The expenses caused by planned standstills for the purpose of corrosion inspection and potential repairs of the corrosion-affected structural elements and orders of magnitude lower than direct and indirect expenses caused by the accidental destruction [22].

ACKNOWLEDGMENT

This work is supported by the Ministry of Science, Technological Development and Innovation of the Republic of Serbia (contracts 451-03-137/2025-03/ 200105, 451-03-136/2025-03/200105 and 451-03-136 /2025-03/ 20021).

REFERENCES

[1] *Stacking, blending, reclaiming of bulk materials*, Wöhlbier, R.H. (Ed.), Trans Tech Publications, Clausthal-Zellerfeld, 1977.

[2] Durst, W., Vogt, W.: *Bucket Wheel Excavator*, Trans Tech Publications, Clausthal-Zellerfeld, 1989.

[3] Moczko, P., Pietrusiak, D., Rusiński, E.: Mate–rial handling and mining equipment – Inter–national standards recommendations for design and testing, FME Transactions, Vol. 46, No. 3, pp. 291-298, 2018.https://www.mas.bg.ac.rs /_media/istraziva nje/fme/vol46/3/1_pmoczko_et_al.pdf

[4] Fleming, M.: Following failure to success - An interview with Charles Rau, J. Fail. Anal. Prev, Vol. 1, No. 1, pp. 18-24, 2001. https://doi.org/ 10.1007/s11668-006-5006-3

[5] Field Engineers. Case study - Conveyor bridge collapse. https://www.fieldengineers.com.au/ case-studies/conveyor-bridge-collapse-at-a-goulburn-nsw-quarry/

[6] Krige, G.J.: Learning from structural failures of materials handling equipment, in: *Australasian structural engineering conference 2012: The past, present and future of structural engineering*, Engineers Australia, Barton, pp. 130–137. https://search.informit.org/doi/10.3316/in formit.026293678460196

[7] Schmidt, M.J., van Rensburg, B.W.J.: Avoiding structural failures on mobile bulk materials handling equipment, J. South. Afr. Inst. Min. Metall, Vol. 115, No. 3, pp. 179-184, 2015. http://www.scielo.org.za /scielo.php?script=sciarttext&pid=S2225-62532 015000300004&lng=en &tlng=en

[8] Taylor, T.M.: Simultaneous collapse of three raw coal conveyors at the largest underground coal mining complex in North America, in: *Structures congress 2018: Blast, impact loading, and response; and research and education*, American Society of Civil Engineers, Reston, pp. 481-492. https://ascelibrary.org/doi/10.1061/97807844813 49.046

[9] Moczko, P., Pietrusiak, D., Wieckowski, J.: Investigation of the failure of the bucket wheel excavator bridge conveyor, Eng. Fail. Anal, Vol. 106, Paper 104180, 2019. https://doi. org/10.1016/j.engfailanal.2019.104180

[10] Bošnjak, S., Arsić, M., Zrnić, N., Rakin, M., Pantelić, M.: Bucket wheel excavator: Integrity assessment of the bucket wheel boom tie-rod welded joint, Eng. Fail. Anal, Vol. 18, No 1, pp. 212–222, 2011. https://doi.org/10.1016/j. engfailan al.2010.09.001

[11] Žužek, B., Burja, J.: Failure of a coal trans–portation conveyor belt pulley, Eng. Fail. Anal, Vol. 106, Paper 104143, 2019. https://doi.org/ 10.1016/j.engfailanal.2019.08.009

[12] Vasić, M., Stojanović, B., Blagojević, M.: Failure analysis of idler roller bearings in belt conveyors, Eng. Fail. Anal, Vol. 117, Paper 104898, 2020. https://doi.org/10.1016/j.engfail anal.2020.104898

[13] Mukhopadhyay, G.: Construction failures due to improper materials, manufacturing, and design, in: Makhlouf, A.S.H., Aliofkhazraei, M. (Eds.): *Handbook of Materials Failure Analysis*, Butterworth-Heinemann, Oxford, pp. 59-81, 2018. https://doi.org/10.1016/B978-0-08-101928-3.00 004-5

[14] Ravikumar, S., Kanagasabapathy, H. and Muralidharan, V.: Multi-component fault diagnosis of self aligning troughing roller (SATR) in belt conveyor system using decision tree - A statistical approach, FME Tran–sactions, Vol. 48, No. 2, pp. 364-371, 2020. https://www.mas. bg.ac.rs/media/istrazivanje/fme/vol48/2/14_v._m uralidharan_et_al..pdf

[15] Bortnowski, P., Kawalec, W., Król, R., Ozdoba, M.: Types and causes of damage to the conveyor belt - Review, classification and mutual relations, Eng. Fail. Anal, Vol 140, Paper 106520, 2022. https://doi.org/10.1016/j. engfailanal.2022.106520

[16] Andrejiova, M., Grincova, A., Marasova, D.: Measurement and simulation of impact wear damage to industrial conveyor belts, Wear, Vol. 368-369, pp. 400-407, 2016. https://doi.org/ 10.1016/j.wear.2016.10.010

[17] Zamiralova, M.E., Lodewijks, G.: Shape sta–bility of pipe belt conveyors: From throughability to pipe-ability, FME Transactions, Vol. 44, No. 3, pp. 263-271, 2016. https:// www.mas.bg.ac.rs/media/ istrazivanje/fme/vol44/3/6_mzamiralova_et_al.pdf

[18] Bugaric, U., Tanasijevic, M., Polovina, D., Ignjatovic, D., Jovancic, P.: Lost production costs of the overburden excavation system caused by rubber belt failure, Eksploat. i Niezawodn, Vol 14, No. 4, pp. 333–341, 2012. https://archive.ein.org.pl /sites/default/files/2012-04-10.pdf

[19] Pantelić, M., Bošnjak, S., Misita, M., Gnja–tović, N., Stefanović, A.: Service FMECA of a bucket wheel excavator, Eng. Fail. Anal, Vol 108, Paper 104289, 2020. https://doi.org/10. 1016/j.engfailanal.2019.104289

[20] Gagg, C., Lewis, P.: Environmentally assisted product failure - Synopsis and case study compendium, Eng. Fail. Anal, Vol. 15, No. 5, pp. 505-520, 2008. https://doi.org/10.1016/j. engfailanal.2007.05.001

[21] Geary, W., Hobbs, J.: Catastrophic failure of a carbon steel storage tank due to internal cor–rosion, Case Stud. Eng. Fail. Anal, Vol. 1, No 4, pp. 257-264, 2013. https://doi.org/10.1016/ j.csefa.2013.09.002

[22] Roberge, P.: *Corrosion engineering – Principles and practice*, McGraw-Hill, New York, 2008.

[23] SRPS EN ISO 12944-2:2018, *Paints and var–nishes - Corrosion protection of steel structures by protective paint systems - Part 2: Classification of environments*, Institute for Standardization of Serbia, Belgrade, 2018.

[24] SRPS EN ISO 14284: *Steel and iron – Sampling and preparation of samples for the determination of chemical composition*, Institute for Standardization of Serbia, Belgrade, 2022.

[25] ISO 14707: *Surface chemical analysis - Glow discharge optical emission spectrometry (GD-OES) - Introduction to use*, ISO - International Organization for Standardization, Geneva, 2021.

[26] SRPS EN ISO 6892-1: *Metallic materials - Tensile testing - Part 1: Method of test at room temperature*, Institute for Standardization of Serbia, Belgrade, 2020.

[27] SRPS EN ISO 148-1: *Metallic materials - Charpy pendulum impact test - Part 1: Test method*, Institute for Standardization of Serbia, Belgrade, 2017.

[28] SRPS EN 10025-1: *Hot rolled products of structural steels - Part 1: General technical delivery conditions*, Institute for Standardization of Serbia, Belgrade, 2011.

[29] SRPS EN ISO 6507-1: *Metallic materials - Vickers hardness test - Part 1: Test method*, Institute for Standardization of Serbia, Belg–rade, 2018.

[30] Szala, M., Szafran, M., Macek, W., Marchenko, S., Hejwowski, T.: Abrasion resistance of S235, S355, C45, AISI 304 and Hardox 500 steels with usage of garnet, corundum and carborundum abrasives, Adv. Sci. Technol. Res. J, Vol 13, No. 4, pp. 151-161, 2019. https://doi.org/10.12913/22998624/ 113244

[31] Pavlina, E., van Tyne, C.: Correlation of yield strength and tensile strength with hardness for steels, J. Mater. Eng. Perform, Vol. 17, No 6, pp. 888-893, 2008. https://doi.org/10.1007/ s11665-008-9225-5

[32] Almeida, S.M., Lage, J., Fernández, B., Garcia, S., Reis, M.A., Chaves, P.C.: Chemical cha–racterization of atmospheric particles and source apportionment in the vicinity of a steelmaking industry, Sci. Total. Environ, Vol. 521-522, pp. 411-420, 2015. http://dx.doi.org /10.1016/j. scitotenv.2015.03.112

[33] Koponen, M., Gustafsson, T., Kalliomäki, K., Kalliomäki, P.-L., Moilanen, M., Pyy, L.: Dusts in a steel-making plant, Int. Arch. Occ. Env. Hea, Vol. 47, No. 1, pp. 35-45, 1980. https://doi.org/10.1007/BF00378326

[34] Birat, J.-P.: Society, Materials, and the Envi–ronment: The case of steel, Metals-Basel, Vol. 10, No. 3, Paper 331, 2020. https://doi.org /10.3390/met10030331

[35] Kamimura, T., Nasu, S., Tazaki, T., Kuzushita, K., Morimoto, S.: Mössbauer spectroscopic study of rust formed on a weathering steel and a mild steel exposed for a long term in an industrial environment, Mater. Trans, Vol 43, No. 4, pp. 694-703. 2002. https://doi.org/10. 2320/matertrans.43. 694

[36] Gomaa, S., El-Hossieny, O., Alnaggar, M.: Effects of mill scale and varying exposure conditions on corrosion behavior of A572 structural steel, Constru. Build. Mater, Vol. 440, Paper 136995, 2024. https://doi.org/10.1016/j. conbuildmat.2024. 136995

[37] Chen, T., Sun, L., Li, Q., Liu, C., Liu, Z., Cheng, X., Li, X.: Comprehensive analysis of corrosion failure of blast furnace gas pipeline in a steel plant, Eng. Fail. Anal, Vol. 154, Paper 107651. 2023. https://doi.org/10.1016/ j.engfailanal.2023.107651

[38] *Steel designers' manual*, Davison, B., Owens, G.W. (Eds.), Steel Construction Institute, Wiley-Blackwell, Chichester, 2016.

[39] EN 1991-1-3: Eurocode 1: *Action on structures - Part 1-3: General actions - Snow loads*, European Committee for Standardization, Brussels, 2003.

[40] Bošnjak, S., Arsić, M., Savićević, S., Milojević, G. Arsić, D.: Fracture analysis of the pulley of a bucket wheel boom hoist system, Eksploat. i Niezawodn, Vol. 18, No. 2, pp. 155-163, 2016. http://dx.doi.org/10.17531/ein. 2016.2.1

[41] Morgan, R., Gatto, F., Biggs, M.: Bulk handling equipment - replacement vs refurbishment. Aspec Engineering Pty, 2020. https://aspec. com.au/ app/uploads/2020/08/Article-Replace ment-vs-refurbishment-20082020-RM.pdf

[42] Han, W., Pan, C., Wang, Z., Yu, G.: Initial atmospheric corrosion of carbon steel in indus–trial environment, J. Mater. Eng. Perform, Vol. 24, No. 2, pp 864-874, 2015. https://doi.org/ 10.1007/s11665-014-1329-5

[43] Zhang, J.-Z., He, Y.-H., Zhang, W.-J., Zhang, P., Wang, Y.-Z., Li, G.-Q.: Yield resistance and ultimate resistance of steel beam with random corrosion damage, Int. J. Steel Struct, Vol. 24, No.

3, pp. 579-590, 2024. https://doi .org/10.1007/ s13296-024-00838-3

[44] Landolfo, R., Cascini, L., Portioli, F.: Modeling of metal structure corrosion damage: A state of the art report, Sustainability, Vol. 2, No. 7, pp. 2163-2175, 2010. https://doi.org/10. 3390/su2072163

[45] Cerit, M., Genel, K., Eksi, S.: Numerical in–vestigation on stress concentration of corrosion pit, Eng. Fail. Anal, Vol.16, No. 7, pp. 2467-2472, 2009. https://doi.org/10.1016/j.engfail anal.2009. 04.004

[46] Cerit, M., Kokumer, O., Genel, K.: Stress con–centration effects of undercut defect and rein–forcement metal in butt welded joint, Eng. Fail. Anal, Vol. 17, No. 2, pp. 571-578, 2010. https: //doi.org/10.1016/j.engfailanal.2009.10.010

[47] Wang, Y., Kong, Z., Xu, S.: Hysteresis perfor–mance of steel beam-column welded T-joints corroded in steel industrial atmosphere, Eng. Fail. Anal. Vol. 159, Paper 108118, 2024. https ://doi.org/10.1016/j.engfailanal.2024.108118

[48] Bakić, G.M., Šijački Žeravčić, V.M., Đukić, M.B. and Anđelić, B.M.: Probability of failure of thermal power plant boiler tubing system due to corrosion, FME Transactions, Vol. 35, No. 1, pp. 47-54, 2007. https://www.mas.bg. ac.rs/_media/ istrazivanje/fme/vol35/1/8._gordana_bakic_4754.pdf

[49] Khalaf, A.H., et al.: Emerging AI techno–logies for corrosion monitoring in oil and gas industry: A comprehensive review, Eng. Fail. Anal, Vol. 155, Paper 107735, 2024. https ://doi.org/10.1016/j. engfailanal.2023.107735

[50] Rusiński, E., Czmochowski, J., Moczko, P. and Pietrusiak, D.: Challenges and strategies of long-life operation and maintenance of tech–nical objects, FME Transactions, Vol. 44, No. 3, pp. 219-228, 2016. https://www.mas.bg.ac. rs/_media/ istrazivanje/fme/vol44/3/1_erusinski_et_al.pdf

КОЛАПС КОСОГ ТРАНСПОРТНОГ МОСТА ИЗАЗВАН КОРОЗИЈОМ

С.М. Бошњак, Д.Б. Момчиловић, Н.Б. Гњатовић, А.З. Стефановић, М.М. Урошевић, И.Љ. Миленовић

У раду су изложени резултати холистичке анализе основног узрока изненадног колапса косог транспортног моста (КТМ), који представља витални подсистем система унутрашњег транспорта железаре. Свеобухватном анализом скупа могућих узрока (грешке у пројектовању, грешке у произ–водњи, грешке у експлоатацији и екстремни утицаји радне околине), методом елиминације утврђено је да је лоше одржавање антикорозионе заштите основни узрок колапса КТМ. Управо због тога, врло изра–жена униформна корозија, потенцирана повећаном киселошћу падавина на подручју железаре, довела је до дезинтеграције елемената конструкције и колапса КТМ. На основу изгледа и положаја скршених остатака КТМ, као и стања објеката које је пре хаварије повезивао, установљен је и презентиран сценарио колапса КТМ. Изложени резултати истра–живања указују на значај мониторинга и контроле стања антикорозионе заштите, посебно када је реч о постројењима изложеним утицају хемијски агресивне околине. Трошкови изазвани планским застојима ради контроле стања антикорозионе заштите и евентуалним санацијама корозијом оштећених елемената носеће конструкције, вишеструко су нижи од директних и индиректних трошкова изазваних изненадним акцидентима.